

Mechanically Interlocked Chiral Self-Templated [2] Catenanes from 2,6-Bis(1,2,3-triazol-4-yl)pyridine (btp) Ligands

Eoin P. McCarney,^{*,[a]} June I. Lovitt,^[a] and Thorfinnur Gunnlaugsson^{*,[a]}

In loving memory of Paddy McCarney

Abstract: We report the efficient self-templated formation of optically active 2,6-bis(1,2,3-triazol-4-yl)pyridine (**btp**) derived homocircuit [2]catenane enantiomers. This represents the first example of the enantiopure formation of chiral **btp** homocircuit [2]catenanes from starting materials consisting of a classical chiral element; X-ray diffraction crystallography enabled the structural characterization of the [2]catenane. The self-assembly reaction was monitored closely in solution facilitating the characterization of the *pseudo*-rotaxane reaction intermediate prior to mechanically interlocking the pre-organised system via ring-closing metathesis.

Molecular chirality presents a decisive challenge in host-guest recognition, asymmetric catalysis, etc.^[1–2] Recently attention has been turned towards development of 3D scaffolds such as chiral interlocked systems which are utilised both as efficient enantioselective receptors and in the formation of molecular machines, knots, etc.^[3–4] Mechanically interlocked molecules, either possessing an inherent chirality arising from the precursors,^[5] or acquiring chirality as a result of the mechanical bond (mechanically planar chiral), have been reported.^[6–7] However, to the best of our knowledge, there are no reports of chiral self-templated homocircuit [2]catenanes from starting materials possessing a classical chiral element, for example a chiral centre. The terdentate heteroaromatic 2,6-bis(1,2,3-triazol-4-yl)pyridine (**btp**) motif has featured frequently in the

literature in recent times.^[8] We have investigated the chemistry of symmetrical **btp** ligands with various *d*-,^[9] and *f*-metal ions,^[10] in the formation of stimuli-responsive gels^[11] and as luminescent cation exchange MOF materials.^[12] We recently also reported the ability of **btp** to self-template, via hydrogen bonding, and employed this feature in the formation of interlocked [2]catenanes; that were employed as selective receptors for phosphate.^[13] Here we show that using a chiral **btp** core possessing two stereogenic centres (*R,R* or *S,S*) in combination with the self-templated strategy, and a double ring-closing metathesis (RCM), the formation of homocircuit mechanically interlocked systems, with chiroptical properties, can be achieved, Scheme 1. We also demonstrate that the formation of such chiral [2]catenanes can be accomplished via an initial *pseudo*-rotaxane formation, followed by the RCM reaction.

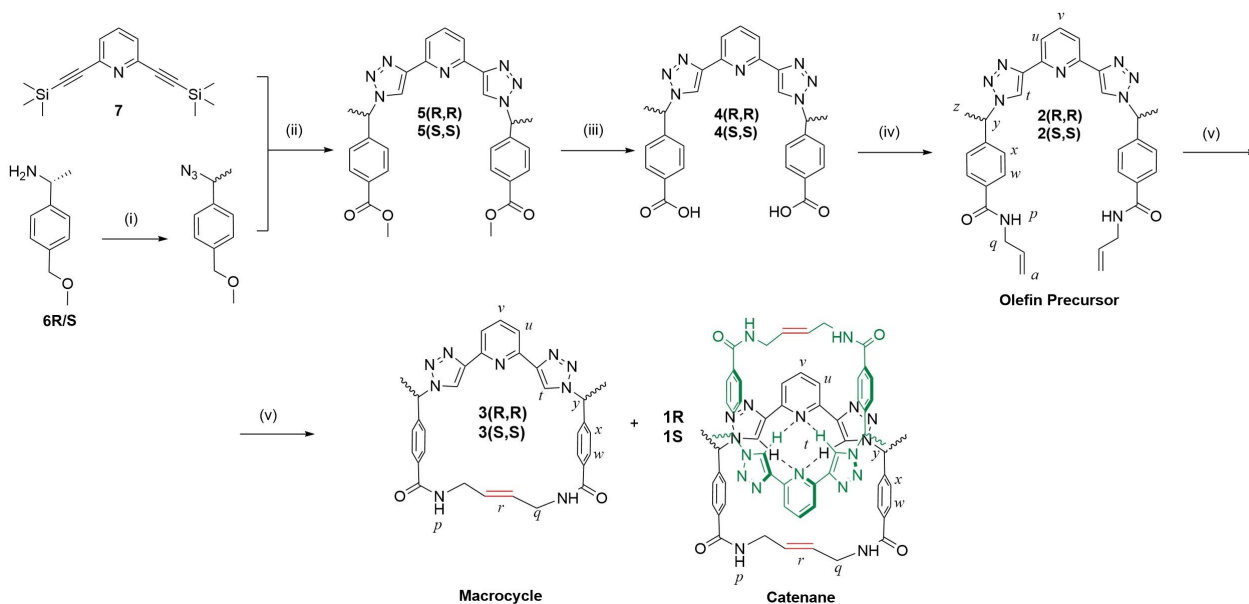
The **btp** ligands **1R/S**, functionalised at the *N1* triazolyl positions with point chirality, were synthesised according to Scheme 1 (see the Supporting Information for more details and characterisation of all intermediates and products). Unlike what was previously reported^[13] in which the precursors were only soluble in DMSO, the introduction of the chiral methyl groups in **2R/S** resulted in dramatically improved solubility in solvents such as CH₂Cl₂ and CHCl₃. As is evident from ¹H NMR titration analysis (see the Supporting Information), this promoted stronger hydrogen bonding interactions, which facilitated the formation of the desired self-templating precursors (as depicted in Scheme 1) through hydrogen bonding of *anti-anti* oriented **btp** motifs (Scheme 1).^[14]

Initially, the RCM synthesis of the [2]catenane **1(S,S)** was deemed to be successful by ¹H NMR. However, the crude ¹H NMR also showed the formation of small amounts of epimers, one of which crystallised. Analysis showed that the root to this epimerisation laid in the previous hydrolysis of **5(S,S)** (see Scheme 1) at elevated temperatures, and was not due to the formation of the interlocked molecule **1S** itself. Hence, carrying out the hydrolysis of **5(S,S)** at ambient temperature using stoichiometric amount of NaOH, circumvented this problem, and the CD spectra of **4(S,S)** and **4(R,R)** gave rise to spectra with equal but opposite dichroism bands, which is consistent with the presence of a single chiral stereoisomer in solution for these two ligands, respectively (at elevated temperature prolonged heating resulted in loss of the CD signature demonstrating the formation of racemates, c.f. Supporting Information). Hence, by using this modified procedure, the

[a] Dr. E. P. McCarney, J. I. Lovitt, Prof. T. Gunnlaugsson
School of Chemistry,
and SFI Synthesis and Solid State Pharmaceutical Centre (SSPC)
Trinity Biomedical Sciences Institute (TBSI)
Trinity College Dublin
The University of Dublin, Dublin 2 (Ireland)
E-mail: mccarney@tcd.ie
gunnlaut@tcd.ie
Homepage: <http://thorrigunnlaugsson.wordpress.com>

Supporting information for this article is available on the WWW under <https://doi.org/10.1002/chem.202101773>

© 2021 The Authors. Published by Wiley-VCH GmbH. This is an open access article under the terms of the Creative Commons Attribution Non-Commercial NoDerivs License, which permits use and distribution in any medium, provided the original work is properly cited, the use is non-commercial and no modifications or adaptations are made.



Scheme 1. Synthesis of chiral **btp** ligands **1R/S**. (i) $\text{CuSO}_4 \cdot 5\text{H}_2\text{O}$, $\text{ImSO}_2\text{N}_3 \cdot \text{H}_2\text{SO}_4$ and K_2CO_3 in CH_3OH , rt, 15 h; (ii) Sodium ascorbate, K_2CO_3 , DMF/ $t\text{BuOH}/ \text{H}_2\text{O}$ (5:5:3), rt, 18 h; (iii) $\text{NaOH}_{(\text{aq})}$, MeOH, rt, 17 h (iv) 1) Et_3N , DMAP, $\text{CH}_2\text{Cl}_2/ \text{DMF}$ (4:1), 0°C , 30 mins 2) EDCI-HCl, 0°C , 30 mins, rt, 66 h. (v) Hoveyda-Grubbs 2nd Gen. Catalyst, DCM (anhydrous), rt, 7 days.

formation of enantiomerically pure forms of the [2]catenanes **1(S,S)** and **1(R,R)** was successfully achieved, through stirring a solution containing **2R/S** and Hoveyda-Grubbs 2nd generation catalyst in anhydrous CH_2Cl_2 under argon at room temperature in darkness for 7 days, before purification of the reaction mixture by flash chromatography.

The [2]catenanes **1R/S** were obtained in yields of 42% and 43% for **1R/S**, respectively, which is similar to that seen for the achiral [2]catenane previously developed in our laboratory,^[13] indicating the chiral groups do not affect the efficiency of the catenation step. The by-products of the synthesis **1R/S** (Scheme 1) were the corresponding macrocycles **3R/S**, which were also isolated during the flash chromatography purification of **1R/S** (see Supporting Information for details). The low isolated yield of both enantiomers, 8% and 14% for **3(R,R)** and **3(S,S)**, respectively, was evidence that the [2]catenane formation is favoured in these cases (*c.f.* ^1H NMR of **3(R,R)** and **3(S,S)**, shown in Figures S10/S11, as well as Figure 4 for **3(S,S)** Supporting Information).

For both enantiomers **1R/S**, resonances indicative of [2] catenane formation were observed by ^1H NMR, Figure 1. The resonances assigned to the aryl rings were heavily shielded, the two resonances moving from 7.86 and 7.43 ppm for **2(R,R)** to 7.26 and 6.32 ppm for **1(R,R)** (*w* and *x*, respectively). This was indicative of a freely-rotating mechanically interlocked structure, where the protons of one ring were able to reside in close proximity to the aromatic rings of the other macrocycle.^[15] Furthermore, weak through-space interactions between the aryl rings and the **btp** motif were observed using ROESY NMR spectroscopy (Figure S12, Supporting Information), which was consistent with formation of the desired interlocked species. ROESY NMR experiments indicated the presence of a stronger

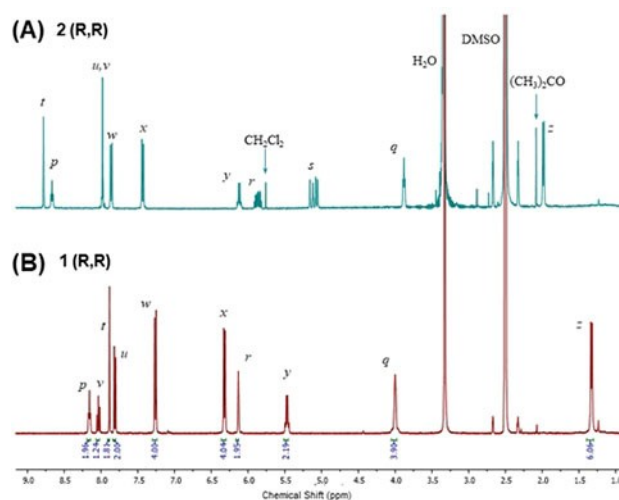


Figure 1. ^1H NMR spectra of chiral **btp** olefin precursor **2(R,R)** (A) and chiral **btp** [2]catenane **1(R,R)** (B) (400 MHz, $\text{DMSO}-d_6$) with resonances labelled.

through-space interaction between aryl protons *w* and pyridyl protons *u* compared with that seen for aryl protons labelled *x* and the latter. Aryl protons *w* also interacted more strongly than aryl protons *x* with pyridyl proton *v* indicating a closer proximity of that end of the aryl aromatic rings with the **btp** motif. In contrast, then by using a less polar solvent, the ^1H NMR of [2]catenane **1R/S** in CDCl_3 displayed pronounced broadening of particular proton resonances (Figure S26). The broadened nature of the triazolyl (*t*), aryl (*x*), methine (*y*) and methyl (*z*) proton resonances, and to a lesser extent the pyridyl resonances (*u* and *v*), indicated some fluxional processes arising as a result of the movement of the component macrocycles

relative to each other.^[15] The formation of the [2]catenane was further confirmed by the appearance of characteristic peaks upon HRMS analysis. The MALDI⁺ spectra showed peaks at $m/z = 1141.4824$ and $m/z = 1141.4813$ corresponding to the $[M + H]^+$ species for **1(R,R)** and **1(S,S)**, respectively.

When the RCM was carried out using a 1:1 mixture of **2R/S** and the epimer **2(R,S)**, a mixture of interlocked systems were produced, giving rise to a complex ¹H NMR spectrum (See Supporting Information). The mixture consisted of a potential number of components such as enantiomers **1R** and **1S**, and their diastereomers **1(R,R)(S,S)**, **1(R,R)(R,S)**, **1(R,R)(S,R)**, **1(S,S)(R,S)** and **1(S,S)(S,R)**. The different orientations of the methyl groups of diastereomers **1(R,R)(R,S)** and **1(R,R)(S,R)**, for example, when closely packed in their respective [2]catenane systems transferred notably different chemical environments to their protons resulting in groups of overlapping multiplet resonances. In particular, resonances associated with the **btp** motif and adjacent chiral centres were widely dispersed, whereas resonances such as *w*, *r*, *q* and to a lesser extent *x*, were concentrated in narrower chemical shift ranges (c.f. Figure 1 for numbering, and Supporting Information for NMR of the products). This was evidence that the self-templated [2]catenane formation was not affected by the presence of the chiral centre as enantiomers and diastereomers alike templated the formation of mixed mechanically interlocked systems under the same reaction conditions used to obtain the enantiopure homocircuit [2]catenanes. No evidence of self-sorting was observed.

The photophysical properties of **2R/S**, **1R/S**, as well as of the macrocycles **3R/S**, were also investigated and the UV-Vis absorption spectra of **2R/S** and **1R/S** are shown in Figure 2A (c.f. also Supporting Information). As discussed above for **5(S,S)** and **5(R,R)**, the introduction of chiral centres in close proximity to the **btp** moieties results in chiroptical activity.^[10,14a] This allowed us to observe the effect of the stereochemistry in the

spectroscopic properties of **2R/S** (see the Supporting Information) and in the resulting chiral [2]catenane products **1R/S**. Indeed the CD analysis showed that the self-templated synthesis of [2]catenanes from **2R/S** gave indeed rise to the formation of **1R/S** as pair of enantiomers, Figure 2B. This analysis also showed that there was a dramatic difference in the CD spectra of **1R/S** vs. that seen for the **btp** precursors **2R/S** (see Figure S23, Supporting Information), demonstrating that the two systems had clear chiral and distinguishable signatures.

The CD spectra of **1R/S** are shown in Figure 2B, exhibiting CD-signals of opposite signs of equal magnitude;^[16] and display the Cotton effect in both of the bands centred at 231 nm and 306 nm, respectively. This due to an exciton coupling between the chromophores of similar energy in close proximity, brought together by the self-templated [2]catenane formation. In the case of **1(S,S)** a large positive exciton couplet with a Davydov splitting of ca. 20 nm, arising from splitting of the 306 nm-centred **btp** $n \rightarrow \pi^*$ transition was observed. The Cotton effect was also observed in the 231 nm centred $\pi \rightarrow \pi^*$ transition. In this case, an exciton couplet with a Davydov splitting of ca. 15 nm, was observed also arising due to the close proximity of the aromatic rings as a result of the [2]catenane formation.

The formation of the [2]catenane was also confirmed by single crystal X-ray diffraction analysis (All crystal structure refinement details are provided in Table S1).^[17] We were unable to obtain suitable crystals from the enantiomerically pure forms of **1(R,R)** or **1(S,S)**. However, blade-like single crystals were obtained by slow evaporation of a solution consisting of CH₃OH:CH₂Cl₂ (9:1) from the epimerised mixture of the [2]catenane '**1S**' discussed above. The data was solved and refined in the triclinic *P*-1 space group with one crystallographically distinct molecule in the asymmetric unit, see Figure 3. The asymmetric unit also contained a number of partially occupied methanol solvent molecule clusters. *P*-1 was used to retain the data:parameter ratio and keep $Z' = 1$ in order to avoid correlations on the atomic displacement parameters (ADPs) of the *pseudo*-equivalent atoms, accepting that no information could be extracted about the relative or absolute stereochemistry in either case. The resulting molecular structure (**1**) is shown in Figure 3, demonstrating that the successful formation of the mechanical bond does not give rise to topological chirality due to the symmetric nature of the component macrocycles ensuring there is no directionality in their rings after RCM unlike other homocircuit systems.^[7]

The crystal structure is worth further commenting on as there exists a number of intramolecular hydrogen bonding interactions. This includes a pair of hydrogen bonding interactions per interlocked macrocycle between **btp** motifs, directed to the pyridyl nitrogen atom acceptor of one constituent molecule from each triazolyl *CH* donor of the other interlocked constituent macrocycle. Hence, in these, each pair of triazole donors binds to the pyridine acceptor of the other catenane 'thread'. The geometry of this hydrogen bonding moiety is *pseudo*-octahedral with the pyridyl nitrogen atoms of opposite macrocycles occupying the polyhedron apices and the triazolyl hydrogen atoms occupying the equatorial positions with hydrogen bonding distances ($|C_{\text{triaz}} - N_{\text{pyr}}|$) of ~ 3.5 Å and

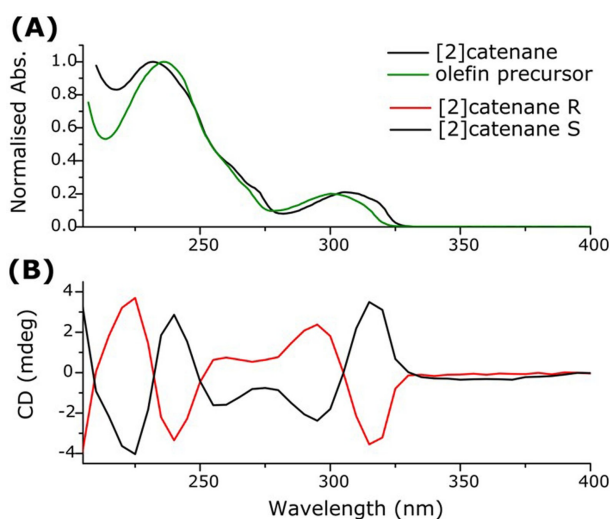


Figure 2. Photophysical spectra of ligands olefin precursor **2R/S** and [2]catenane **1R/S** measured in CH₃CN at room temperature ($c = 1 \times 10^{-5}$ M): (A) UV-vis absorption spectra comparison of **2R/S** and **1R/S**; (B) CD spectra of **1R/S**.

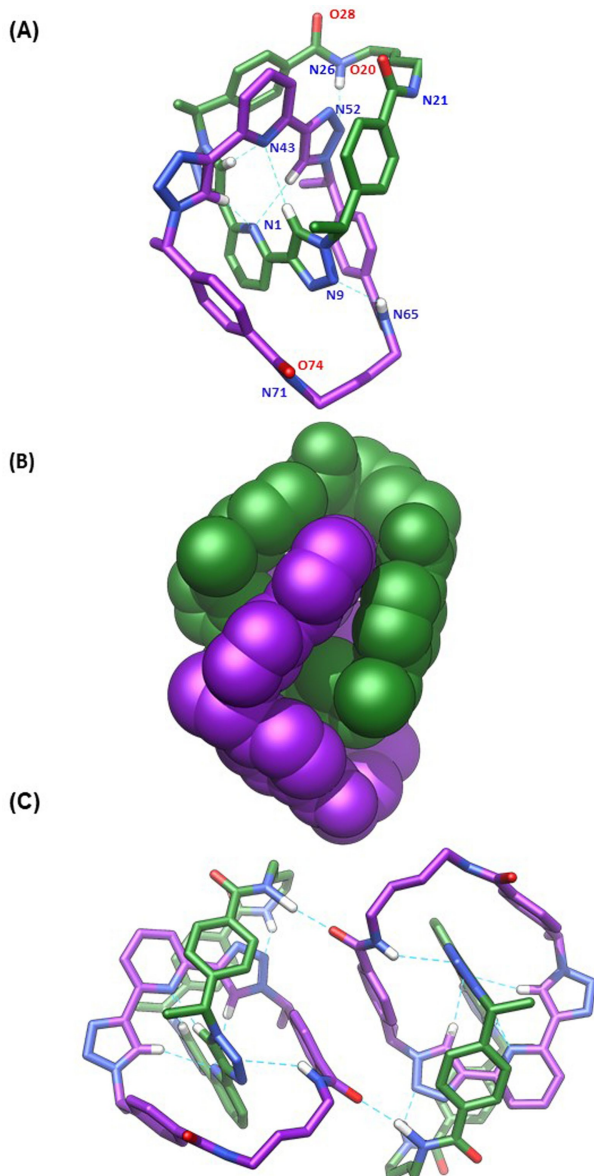


Figure 3. (A) Perspective view of the molecular structure of [2]catenane 1. Selected heteroatom labelling shown. Disordered contributor, selected hydrogen atoms and solvent molecules omitted for clarity. (B) Spacefill representation of [2]catenane 1. (C) Extended structure of [2]catenane 1 illustrating hydrogen bonding interactions between adjacent moieties.

angles $\angle(C-H\cdots N)$ of $\sim 170^\circ$ (see Table S2, Supporting Information). The *pseudo*-octahedral polyhedron of the **btp**-**btp** hydrogen bonding moiety arises as a result of the planar **btp** motifs oriented essentially orthogonally to each other (the angle between the mean planes of the **btp** motifs is 97.5°). Significant π - π stacking is observed as the two aryl rings of both constituent macrocycles overlap with the pyridine-triazole unit of the **btp** motifs of the opposite constituent macrocycles. Thus, the four of these stacking interactions have perpendicular plane to plane centroid distances of between 3.4 \AA – 3.8 \AA and angles between mean plane normals ranging from 11.9° – 23.2° . The stacking behaviour seen in the solid-state structure is consistent

with the weak through-space interactions between the aryl rings and the **btp** motif observed using ROESY NMR spectroscopy, discussed earlier.

The extended structure is supported through various networks of hydrogen bonding interactions between one triazolyl nitrogen atom acceptor per [2]catenane constituent molecule and the amide nitrogen atom hydrogen bond donor on its interlocked equivalent. One of the hydrogen bonding interactions is between the cisoid amide N26 donor and the medial triazolyl nitrogen atom N52 of the other macrocycle. Here the distance $|N-H\cdots N|$ is $3.239(1) \text{ \AA}$ and the angle $\angle(N-H\cdots N)$ is $134.4(2)^\circ$. The second hydrogen bonding interaction is between the transoid amide N65 donor of the other macrocycle and the medial triazolyl N9 acceptor of its equivalent consistent interlocked molecule. Hence the distance $|N-H\cdots N|$ is $3.412(1) \text{ \AA}$ and the angle $\angle(N-H\cdots N)$ is 143.7° . There are also intermolecular hydrogen bonding interactions involving the amides. One of the cisoid amides is involved in a pair of hydrogen bonding interactions, firstly a hydrogen bond donor interaction between its NH and O64 oxygen of one of the transoid amides N21 of a neighbouring molecule. The distance $|N-H\cdots O|$ is $2.874(4) \text{ \AA}$ with angle $\angle(N-H\cdots N)$ is $150.4(3)^\circ$.

Having successfully demonstrated the formation of these chiral [2]catenanes, we next investigated if the self-templating effect could also be used in the formation of the *pseudo*-rotaxane and if that product could be converted to the [2]catenane using RCM in situ. To achieve this, a CDCl_3 solution of **2(S,S)** (1.07 mM, 1 mL) as a thread, and a CDCl_3 solution of the macrocycle **3(S,S)** (1.07 mM, 1 mL) were analysed by ^1H NMR, prior to and after mixing, and upon subjecting such a mixture to RCM reaction. The results are shown in Figure 4, showing the aforementioned broadening of certain proton resonances i.e. the triazolyl (*t*) aryl (*x*) and NH (*p*) for **2(S,S)** as shown in Figure 4a, and the sharp resonances observed **3(S,S)** as shown in Figure 4b. The two solutions were then mixed. After initial mixing, all of the relatively sharp proton resonances for **2(S,S)** and **3(S,S)** became broadened. As remarked before, this broadening is indicative of a dynamic fluxional process involving the relative rotation of the self-assembly components, which would indicate the self-association of **2(S,S)** and potential threading of **2(S,S)** through **3(S,S)** to give the *pseudo*-rotaxane, both of which would consist of the hydrogen bonding interactions discussed above.^[15] In fact, (and as shown in Figure 4c) there was no change in this broadening after (stirring for) 120 h, and little information could be gained from the spectrum at room temperature. However, upon carrying out the ^1H NMR experiment at -20°C (as shown in Figure 4d) the resulting spectrum closely began to resemble that observed for the chiral [2]catenane (as shown in Figure 4e), particularly in relation to the proximity of the chemical shifts of the now deshielded olefin proton signal *r*, around 6.2 ppm, and amide proton *p* around 6.7 ppm and of the now shielded aryl signals, *w* and *x*, at 7.3 ppm and 6.3 ppm, respectively. This was strong evidence that the threading of the open form **2(S,S)** through the cavity of the macrocycle **3(S,S)** to yield the desired chiral *pseudo*-rotaxane possessing four stereogenic centres was occurring. Furthermore, the resonances for the **3(S,S)** macrocycle were to

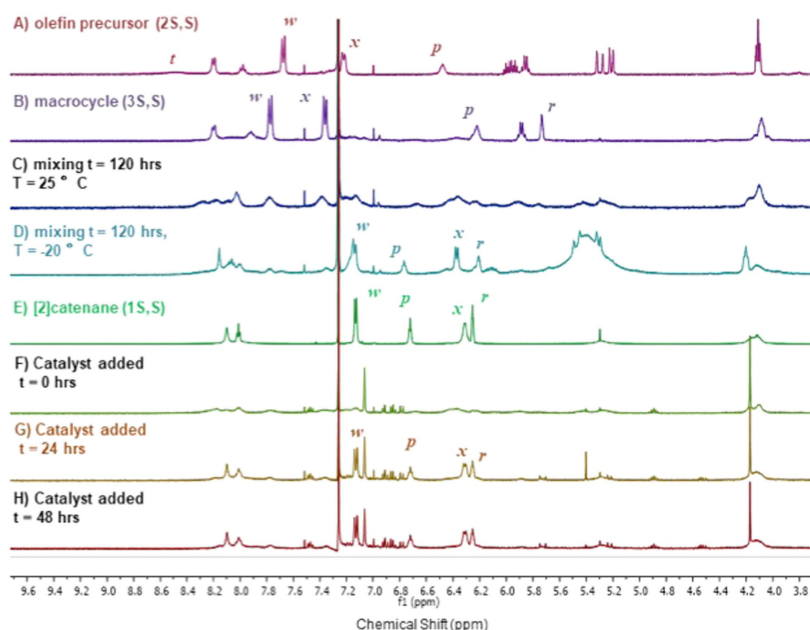


Figure 4. ^1H NMR spectra of the dimerisation of A) **btp** olefin ($2\text{S},\text{S}$) with B) macrocycle ($3\text{S},\text{S}$). C–D) Initial broadening of the proton resonance signals followed by a change in signal chemical shifts, resulting in a spectrum closely resembling that of E) $[2]$ catenane ($1\text{S},\text{S}$), indicated threading of ($2\text{S},\text{S}$) through macrocycle 3S i.e. *pseudo*-rotaxane formation. F–H) Addition of RCM catalyst demonstrated a ^1H spectrum which closely resembled that of the $[2]$ catenane. (enlarged version can be seen in the Supporting Information).

a greater extent absent from the NMR spectrum. Consequently, to this solution, the Hoveyda-Grubbs 2nd generation catalyst was added (0.5 equiv. in CDCl_3) as illustrated in Figures 4f–h and the RCM reaction was followed in situ. Shortly after adding the catalyst, the proton resonances regained their broadened appearance at room temperature. However, after 24 h, a clear resemblance with the NMR spectrum of the $[2]$ catenane was observed, and there was little change to the ^1H NMR spectrum after 48 h. The newly formed olefin proton's signal, *r*, appeared at 6.25 ppm, exactly coincident with the corresponding peak of the $[2]$ catenane $1(\text{S},\text{S})$, while the same observation was made for the amide proton's resonance and the aryl proton's signals, *w* and *x*, at 6.73 ppm, 7.14 ppm and 6.31 ppm, respectively, with no evidence of the appreciative amount of $3(\text{S},\text{S})$ existing in solution.

To further investigate the self-templating effect in the formation of the above *pseudo*-rotaxane (and the $[2]$ catenane) the same in situ ^1H NMR experiment was carried out in $\text{DMSO}-d_6$. We had anticipated that the use of more polar solvent would prevent the self-templating effect, and this was indeed found to be the case, as upon mixing of **btp** olefin $2(\text{S},\text{S})$ and macrocycle $3(\text{S},\text{S})$, no signal broadening, nor any shift in the key resonances was observed, even after 120 h of stirring at room temperature (Figure S12, Supporting Information). In fact, the spectrum after 120 h of mixing $2(\text{S},\text{S})$ and $3(\text{S},\text{S})$ did not resemble that of the $[2]$ catenane (Figure 1) which can be rationalised by the more polar DMSO solvent molecules out-competing the self-templating effect. The threading of $2(\text{S},\text{S})$ through macrocycle $3(\text{S},\text{S})$ is an important step in understanding the process which leads to the formation of self-templated mechanically interlocked **btp** molecules. A process, which can be extended to the formation

of *pseudo*-rotaxanes (as demonstrated here), as well as rotaxanes, and heterocircuit $[2]$ catenane formation. We are currently working on developing such chiral and achiral examples.

Herein, we have demonstrated that the enantiomerically pure **btp** based $[2]$ catenane $1\text{R}/\text{S}$ was successfully formed from the chiral precursors $2\text{R}/\text{S}$, respectively, through the use of self-templated synthesis. Moreover, the mechanical bond did not give rise to topological chirality due to the symmetric nature of the component macrocycles. To the best of our knowledge, the synthesis of $1\text{R}/\text{S}$ represents the first instance of the formation of chiral self-templated homocircuit $[2]$ catenanes from starting materials possessing a classical chiral element.

Experimental Section

Experimental Details can be found in the Supporting Information.

Author Contributions

The manuscript was written through contributions of all authors. The synthesis, characterization and self-assembly studies of the compounds reported were carried out by E.P.M. and J.I.L. T.G. designed and supervised the project with E.P.M. and J.I.L. All authors have given approval to the final version of the manuscript.

Acknowledgements

We would like to thank the Irish Research Council (IRC) for a postgraduate scholarship (to E.P.M. GOIPG/2013/452) and Science Foundation Ireland (SFI) (SFI PI Awards 10/45 IN.1/B2999 and 13/IA/1865 to T.G. and SFI Centre Award for SSPC Research Centres Phase 2 12/RC/2275_P2) for financial support. We would especially like to thank Dr Chris S. Hawes, Keele University, UK, for his continuous support during the development of this project. Open access funding provided by IReL.

Conflict of Interest

The authors declare no conflict of interest.

Keywords: chiral [2]catenanes · chiroptical · interlocked · pre-organisation · self-templated

- [1] a) C. J. Bruns, J. F. Stoddart, *The Nature of the Mechanical Bond: From Molecules to Machines*, Wiley, Hoboken, New Jersey, 2016, p1–p706; b) M. Denis, J. E. M. Lewis, F. Modicom, S. M. Goldup, *Chem* 2019, 5, 1512–1520; c) E. M. G. Jamieson, F. Modicom, S. M. Goldup, *Chem. Soc. Rev.* 2018, 47, 5266–5311; d) K. Nakazono, T. Takata, *Symmetry*. 2020, 12, 144; e) J. P. Carpenter, C. T. McTernan, J. L. Greenfield, R. Lavendomme, T. K. Ronson, J. R. Nitschke, *Chem.* 2021, 5, 1007–1350; f) S.-H. Li, H.-Y. Zhang, X. Xu, Y. Liu, *Nat. Commun.* 2015, 6, 7590.
- [2] a) J. F. Stoddart, *Angew. Chem. Int. Ed.* 2017, 56, 11094–11125; *Angew. Chem.* 2017, 129, 11244–11277; b) J. P. Sauvage, *Angew. Chem. Int. Ed.* 2017, 56, 11080–11093; *Angew. Chem.* 2017, 129, 11228–11242; c) A. Martínez-Cuevas, A. Saura-Sanmartín, M. Alajarin, J. Berna, *ACS Catal.* 2020, 10, 7719–7733; d) W.-J. Li, Q. Gu, X.-Q. Wang, D.-Y. Zhang, Y.-T. Wang, X. He, W. Wang, H.-Bo Yang, *Angew. Chem. Int. Ed.* 2021, 60, 9507–9515; *Angew. Chem.* 2021, 133, 9593–9601; e) N. Pairault, A. Bessaguet, R. Barat, L. Frédéric, G. Pieters, J. Crassous, I. Opalinski, S. Papot, *Chem. Sci.* 2021, 12, 2521–2526; f) M. Galli, J. E. M. Lewis, S. M. Goldup, *Angew. Chem. Int. Ed.* 2015, 54, 13545–13549; *Angew. Chem.* 2015, 127, 13749–13753; g) M. Denis, S. M. Goldup, *Nat. Chem. Rev.* 2017, 1, 0061; h) D. A. Leigh, L. Pirvu, F. Schaufelberger, D. J. Tetlow, L. Zhang, *Angew. Chem. Int. Ed.* 2018, 57, 10484–10488; *Angew. Chem.* 2018, 130, 10644–10648; i) M. Dommaschk, J. Echavaren, D. A. Leigh, V. Marcos, T. A. Singleton, *Angew. Chem. Int. Ed.* 2019, 58, 14955–14958; *Angew. Chem.* 2019, 131, 15097–15100; j) J. Y. C. Lim, I. Marques, V. Félix, P. D. Beer, *Angew. Chem. Int. Ed.* 2018, 57, 584–588; *Angew. Chem.* 2018, 130, 593–597.
- [3] a) J. R. J. Maynard, S. M. Goldup, *Chem.* 2020, 6, 1914–1932; b) N. H. Evans, *Chem. Eur. J.* 2018, 24, 3101–3112; c) N. Pairault, J. Niemeyer, *Synlett* 2018, 29, 689–698; d) J. Crassous, *Chem. Soc. Rev.* 2009, 38, 830–845; e) F. Ishiwari, K. Nakazono, Y. Koyama, T. Takata, *Angew. Chem. Int. Ed.* 2017, 56, 14858–14862; *Angew. Chem.* 2017, 129, 15054–15058; f) T. Morise, A. Muranaka, H. Ban, M. Harada, M. Naito, K. Yoshida, N. Kobayashi, M. Uchiyama, Y. Tokunaga, *Org. Lett.* 2021, 23, 2120–2124; g) D. P. August, S. Borsley, S. L. Cockroft, F. della Sala, D. A. Leigh, S. J. Webb, *J. Am. Chem. Soc.* 2020, 142, 18859–18865; h) D. H. G. David, R. Casares, J. M. Cuerva, A. G. Campana, V. Blanco, *J. Am. Chem. Soc.* 2019, 141, 18064–18074; i) C. E. Gell, T. A. McArdle-Ismaguilov, N. H. Evans, *Chem. Commun.* 2019, 55, 1576–1579.
- [4] a) D. P. August, J. Jaramillo-García, D. A. Leigh, A. Valero, I. J. Vitorica-Yrezabal, *J. Am. Chem. Soc.* 2021, 143, 1154–1161; b) Y. Cakmak, S. Erbas-Cakmak, D. A. Leigh, *J. Am. Chem. Soc.* 2016, 138, 1749–1751; c) G. Bottari, D. A. Leigh, E. M. Perez, *J. Am. Chem. Soc.* 2003, 125, 13360–13361; d) S. Erbas-Cakmak, D. A. Leigh, C. T. McTernan, A. L. Nussbaumer, *Chem. Rev.* 2015, 115, 10081–10206; e) A. Theil, C. Mauve, M.-T. Adeline, A. Marinetti, J.-P. Sauvage, *Angew. Chem. Int. Ed.* 2006, 45, 2104–2107; *Angew. Chem.* 2006, 118, 2158–2161; f) J. Zhong, L. Zhang, D. P. August, G. F. S. Whitehead, D. A. Leigh, *J. Am. Chem. Soc.* 2019, 141, 14249–14256; g) R. S. Forgan, J.-P. Sauvage, J. F. Stoddart, *Chem. Rev.* 2011, 111, 5434–5464.
- [5] a) H. Adams, F. J. Carver, C. A. Hunter, *J. Chem. Soc. Chem. Commun.* 1995, 809–810; b) P. R. Ashton, A. S. Reder, N. Spencer, J. F. Stoddart, *J. Am. Chem. Soc.* 1993, 115, 5286–5287; c) C. P. McArdle, S. Van, M. C. Jennings, R. J. Puddephatt, *J. Am. Chem. Soc.* 2002, 124, 3959–3965; d) C. A. Hunter, *J. Am. Chem. Soc.* 1992, 114, 5303–5311; e) R. Jäger, F. Vögtle, *Angew. Chem. Int. Ed.* 1997, 36, 930–944; *Angew. Chem.* 1997, 109, 9, 966–980; f) S. Ottens-Hildebrandt, M. Nieger, K. Rissanen, J. Rouvinen, S. Meier, G. Harder, F. Vögtle, *J. Chem. Soc. Chem. Commun.* 1995, 777–778; g) A. G. Johnston, D. A. Leigh, R. J. Pritchard, M. D. Deegan, *Angew. Chem. Int. Ed.* 1995, 34, 1209–1212; *Angew. Chem.* 1995, 107, 1324–1327; h) P. R. Ashton, I. Iriepa, M. V. Reddington, N. Spencer, A. M. Z. Slawin, J. F. Stoddart, D. J. Williams, *Tetrahedron Lett.* 1994, 35, 4835–4838; i) M. Asakawa, P. R. Ashton, S. E. Boyd, C. L. Brown, S. Menzer, D. Pasini, J. F. Stoddart, M. S. Tolley, A. J. P. White, D. J. Williams, P. G. Wyatt, *Chem. Eur. J.* 1997, 3, 463–481.
- [6] a) E. A. Neal, S. M. Goldup, *Chem. Commun.* 2014, 50, 5128–5142; b) R. Bordoli, S. M. Goldup, *J. Am. Chem. Soc.* 2014, 136, 4817–4820; c) R. Mitra, H. Zhu, S. Grimme, J. Niemeyer, *Angew. Chem. Int. Ed.* 2017, 56, 11456–11459; *Angew. Chem.* 2017, 129, 11614–11617; d) K. J. Hartlieb, A. K. Blackburn, S. T. Schneebeli, R. S. Forgan, A. A. Sarjeant, C. L. Stern, D. Cao, J. F. Stoddart, *Chem. Sci.* 2014, 5, 90–100; e) A. W. Heard, S. M. Goldup, *Chem.* 2020, 6, 994–1006.
- [7] a) A. Imayoshi, B. V. Lakshmi, Y. Ueda, T. Yoshimura, A. Matayoshi, T. Furuta, T. Kawabata, *Nat. Commun.* 2021, 12, 404; b) P. E. Glen, J. A. T. O'Neill, A.-L. Lee, *Tetrahedron.* 2013, 69, 57–68; c) M. A. Jinks, A. de Juan, M. Denis, C. J. Fletcher, M. Galli, E. M. G. Jamieson, F. Modicom, Z. Zhang, S. M. Goldup, *Angew. Chem. Int. Ed.* 2018, 57, 14806–14810; *Angew. Chem.* 2018, 57, 15022–15026; d) S. Corra, C. de Vet, J. Groppi, M. La Rosa, S. Silvi, M. Baroncini, A. Credì, *J. Am. Chem. Soc.* 2019, 141, 9129–9133; e) C. Tian, S. D. P. Fielden, B. Pérez-Saavedra, I. J. Vitorica-Yrezabal, D. A. Leigh, *J. Am. Chem. Soc.* 2020, 142, 9803–9808; f) M. Gaedke, F. Witte, J. Anhäuser, H. Hupatz, H. V. Schröder, A. Valkonen, K. Rissanen, A. Lützen, B. Paulus, C. A. Schalley, *Chem. Sci.* 2019, 10, 10003–10009.
- [8] a) J. P. Byrne, J. A. Kitchen, T. Gunnlaugsson, *Chem. Soc. Rev.* 2014, 43, 5302–5325; b) M. Ostermeier, M.-A. Berlin, R. M. Meudtner, S. Demeshko, F. Meyer, C. Limberg, S. Hecht, *Chem. Eur. J.* 2010, 16, 10202–10213; c) Y. Li, J. C. Huffman, A. H. Flood, *Chem. Commun.* 2007, 2692–2694; d) Y. Liu, F. C. Parks, W. Zhao, A. H. Flood, *J. Am. Chem. Soc.* 2018, 140, 15477–15486; e) M. Cirulli, A. Kaur, J. E. M. Lewis, Z. Zhang, J. A. Kitchen, S. M. Goldup, M. M. Roessler, *J. Am. Chem. Soc.* 2019, 141, 879–889.
- [9] J. P. Byrne, J. A. Kitchen, O. Kotova, V. Leigh, A. P. Bell, J. J. Boland, M. Albrecht, T. Gunnlaugsson, *Dalton Trans.* 2014, 43, 196–209.
- [10] a) J. P. Byrne, J. A. Kitchen, J. E. O'Brien, R. D. Peacock, T. Gunnlaugsson, *Inorg. Chem.* 2015, 54, 1426–1439; b) S. J. Bradberry, J. P. Byrne, C. P. McCoy, T. Gunnlaugsson, *Chem. Commun.* 2015, 51, 16565–16568.
- [11] E. P. McCarney, J. P. Byrne, B. Twamley, M. Martínez-Calvo, G. Ryan, M. E. Mobius, T. Gunnlaugsson, *Chem. Commun.* 2015, 51, 14123–14126.
- [12] E. P. McCarney, C. S. Hawes, J. A. Kitchen, K. Byrne, W. Schmitt, T. Gunnlaugsson, *Inorg. Chem.* 2018, 57, 3920–3930.
- [13] J. P. Byrne, S. Blasco, A. B. Aletti, G. Hessman, T. Gunnlaugsson, *Angew. Chem. Int. Ed.* 2016, 55, 8938–8943; *Angew. Chem.* 2016, 128, 9084–9089.
- [14] a) J. P. Byrne, M. Martínez-Calvo, R. D. Peacock, T. Gunnlaugsson, *Chem. Eur. J.* 2016, 22, 486–490; b) A. Bosmani, S. A. Pujari, C. Besnard, L. Guenee, A. I. Poblador-Bahamonde, J. Lacour, *Chem. Eur. J.* 2017, 23, 8678–8684.
- [15] C. N. Marrs, N. H. Evans, *Org. Biomol. Chem.* 2015, 13, 11021–11025.
- [16] a) G. Pescitelli, L. Di Bari, N. Berova, *Chem. Soc. Rev.* 2014, 43, 5211–5233; b) N. Berova, L. Di Bari, G. Pescitelli, *Chem. Soc. Rev.* 2007, 36, 914–931.
- [17] Deposition Number 2070472 contains the supplementary crystallographic data for this paper. These data are provided free of charge by the joint Cambridge Crystallographic Data Centre and Fachinformationszentrum Karlsruhe Access Structures service www.ccdc.cam.ac.uk/structures

Manuscript received: May 19, 2021
Accepted manuscript online: June 9, 2021
Version of record online: July 5, 2021